

M.J. Pattison<sup>1</sup>, K.N. Premnath<sup>2</sup>, N.B. Morley<sup>3</sup><sup>1</sup>MetaHeuristics LLC, Santa Barbara, CA 93105, martin@metah.com<sup>2</sup>Department of Chemical Engineering, University of California, Santa Barbara, CA 93105<sup>3</sup>MAE Department, University of California, Los Angeles, CA 90095, morley@fusion.ucla.edu

*Fusion reactors designs frequently involve the use of liquid metal flows in the presence of strong magnetic fields. Simulation of the flows involves the solution of continuum equations for fluid flow and magnetic induction, usually done with finite difference methods. In this paper, an alternative method, based on the generalized lattice Boltzmann equation (GLBE), and implemented in the MetaFlow code is discussed. It has a number of desirable features, including fast execution, excellent parallel scalability, and can easily handle complex geometries. The use of the recent GLBE variant greatly enhances stability and accuracy. To simulate magnetohydrodynamic (MHD) flows relevant to fusion applications using GLBE, several new models have been developed, including new boundary condition formulations, preconditioners for faster steady-state convergence, variable electrical conductivity materials, and to resolve thin Hartmann layers. These models are discussed, and validations against MHD benchmarks, including 3-D driven cavity, high Hartmann number and turbulent cases are presented.*

## I. INTRODUCTION

Most codes used for the simulation of fluid flows solve the equations governing the fluid behavior by using a finite difference or finite volume approach. An alternative methodology, which has gained popularity in recent years, is to use the lattice Boltzmann (LB) method, which is based on kinetic theory. In this approach the fluid at every point on a grid is considered to comprise particle populations with a distribution of different velocities. The general idea behind this scheme is to compute a probability distribution function  $f_\alpha(\mathbf{x}, t)$ , where  $f_\alpha$  is the probability of finding a particle population with velocity  $\mathbf{e}_\alpha$  along the discrete direction  $\alpha$  at location  $\mathbf{x}$  at a particular time  $t$ . A comprehensive review of the lattice Boltzmann method is given by Chen and Doolen<sup>1</sup>, and a brief description is also presented in Section II.

One advantage of the lattice Boltzmann method (LBM) is that it is very well suited to parallel processing on distributed memory architectures. At each time step, it is only necessary for a processor to communicate with a fixed number of other processors, typically between two and eight depending on how the computational domain is divided up. For large problems, the execution speed is roughly proportional to the number of processors used. This contrasts with other methods where each processor has to communicate with all, or many other, processors involved in the computation. In this situation, when large numbers of processors are used, the time spent communicating can become a significant proportion of the overall time, severely reducing the execution speed.

Another benefit is that solution of the Poisson equation is not required in LB methods. Since this takes up 80-90% of the CPU time in traditional solution methods, LB codes are also much faster on a per grid point per time step basis. In addition, LB methods can handle flows in complex geometries relatively without the need for a body fitted grid. The magnetic induction equation can be solved in a similar fashion to the hydrodynamic equations, albeit through a vector LB method, allowing the method to be extended to MHD flows while maintaining the advantageous features of the LB approach.

## II. LATTICE BOLTZMANN METHOD

### II.A. Hydrodynamics

In three dimensional applications of this approach, the calculations are performed on a cubic grid and 15 or 19 velocity models are normally used. In this work, the 19 velocity model was used, due to its superior stability, and this is shown in Fig. 1. The velocity vectors  $\mathbf{e}_\alpha$  correspond to the directions from the centre of the cube to the centers of the edges, from the cube centre to the middle of the faces, with one zero velocity vector. The equations are normally scaled such that in one time step a particle initially at one grid point moves to an adjacent grid point.

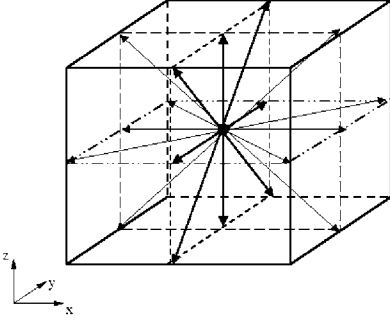


Fig. 1. Three-dimensional nineteen (D3Q19) lattice velocity model.

The basic procedure involved in the LB method is to solve equations for the evolution of a set of distribution functions,  $f_\alpha$  along discrete velocity directions  $\alpha$  from which the macroscopic variables (velocity, pressure etc.) can be recovered. The approach taken here is to use a recent formulation of the LBM, the multiple relaxation time (MRT) model<sup>2,3,4</sup>. This model offers better numerical stability and accuracy than earlier models employing a single relaxation time (SRT).

In the MRT LB method, the equations used for the calculation of  $f_\alpha$  are:

$$\begin{aligned} \tilde{f}_\alpha(\mathbf{x}, t) = & -\sum_{\beta} \Lambda_{\alpha\beta} (f_\beta - f_\beta^{eq}) \\ & + \sum_{\beta} \left( \mathbf{I}_{\alpha\beta} - \frac{1}{2} \Lambda_{\alpha\beta} \right) S_\beta \delta t \end{aligned} \quad (1a)$$

$$f_\alpha(\mathbf{x} + \mathbf{e}_\alpha \delta t, t + \delta t) = \tilde{f}_\alpha(\mathbf{x}, t) \quad (1b)$$

where the summations are over all nineteen directions,  $\alpha$ . The first term on the right hand side of 1a represents the effects of particle collisions;  $f_\alpha^{eq}$  is the equilibrium distribution function and is calculated from the macroscopic flow properties, i.e.

$$f_\alpha^{eq} = f_\alpha^{eq}(\rho, \mathbf{u})$$

where  $\rho$  is the density and  $\mathbf{u}$  the fluid velocity. The tensor  $\Lambda_{\alpha\beta}$  is the relaxation matrix – it is the use of this matrix that distinguishes the MRT from earlier SRT models which instead used a scalar relaxation time. The final term involving  $S_\alpha$  represents the effect of external imposed forces  $F_{ext}$  such as the Lorentz force. The second step, Eq. 1a, represents advection and is known as the streaming step.

The macroscopic properties of the flow can be recovered through the relations

$$\rho = \sum_{\alpha=0}^{18} f_\alpha \quad \rho \mathbf{u} = \sum_{\alpha=0}^{18} \mathbf{e}_\alpha f_\alpha + 1/2 F_{ext} \delta t \quad p = \frac{1}{3} c^2 \rho$$

where  $p$  is the pressure and  $c$  the ratio of the lattice spacing to the time step.

## II.B. Dynamics of Magnetic Induction

The equation for magnetic induction can be solved in a similar manner to the hydrodynamic equations, using a vector distribution function,  $\mathbf{g}$ . The evolution of this function is given by<sup>5</sup>

$$\tilde{\mathbf{g}}_\alpha(\mathbf{x}, t) = \mathbf{g}_\alpha - \frac{1}{\tau_m} (\mathbf{g}_\alpha - \mathbf{g}_\alpha^{eq}) \quad (2a)$$

$$\mathbf{g}_\alpha(\mathbf{x} + \Xi_\alpha \delta t, t + \delta t) = \tilde{\mathbf{g}}_\alpha(\mathbf{x}, t) \quad (2b)$$

A set of seven direction vectors  $\Xi_\alpha$  is used; a zero vector and the six vectors from the cube centre to the middle of the faces in Fig. 1.  $\tau_m$  is a relaxation time which is dependent on the magnetic resistivity and  $\mathbf{g}_\alpha^{eq}$  is an equilibrium distribution function which is a function of the local velocity and the magnetic field  $\mathbf{B}$

$$\mathbf{g}_\alpha^{eq} = \mathbf{g}_\alpha^{eq}(\mathbf{u}, \mathbf{B}). \quad (3)$$

The magnetic field is obtained from the vector distribution function through

$$\mathbf{B} = \sum_{\alpha=0}^6 \mathbf{g}_\alpha \quad (4)$$

The current density can be calculated directly from the moments

$$(\mathbf{J})_k = \frac{-4\epsilon_{ijk}}{c^2 \tau_m \mu_{mag}} \left[ \sum_{\beta=0}^6 \mathbf{e}_{\alpha i} \mathbf{g}_{\beta j} - (\mathbf{u}_i \mathbf{B}_j - \mathbf{B}_i \mathbf{u}_j) \right] \quad (5)$$

where the velocity  $c = \delta x / \delta t$  and  $\epsilon_{ijk}$  is the permutation tensor.

## II.C. Boundary Conditions

For the hydrodynamic equations, boundary conditions at solid walls and the inlet were applied using the interpolated bounce-back scheme<sup>6</sup>. At outlets, an extrapolation scheme<sup>7</sup> was used.

For the induction equation, no suitable formulations for treatment of the boundaries were available in the LBM literature and a new scheme was therefore devised. The approach was similar to the extrapolation scheme used for the fluid flow. A *ghost* layer is introduced around the domain boundary, denoted by the superscript -1 and after performing Eq. 2a but before Eq. 2b, values are calculated through

$$\tilde{\mathbf{g}}_\alpha^{-1} = 2\tilde{\mathbf{g}}_\alpha^0 - \tilde{\mathbf{g}}_\alpha^1 \quad (6)$$

where  $\tilde{\mathbf{g}}_\alpha^0$  and  $\tilde{\mathbf{g}}_\alpha^1$  are the values on the boundary and at one grid spacing inside the boundary, respectively. The magnetic field,  $\mathbf{B}$ , required at the boundary is imposed by using these values to calculate  $\mathbf{g}_\alpha^{eq}$  at the boundary points. Note that this method does not place any restrictions on the electrical conductivity at the boundary.

#### II.D. Low Magnetic Prandtl Number Flows

Most MHD flows of interest involve liquid metals, and for these fluids there is a large difference between the relaxation timescales for the fluid flow and the magnetic induction. The ratio of the timescales varies with the magnetic Prandtl number  $\text{Pr}_m = \nu\sigma\mu_m$  where  $\nu$  is the viscosity,  $\sigma$  is the electrical conductivity and  $\mu_m$  the permeability. For liquid metals,  $\text{Pr}_m \sim 10^{-7}$ . To avoid the large disparity in time steps for the fluid and magnetic equations that would result from this in the solution procedure of LBM, the induction equation is written in the form

$$\frac{\partial \mathbf{B}}{\partial t} + \frac{\chi}{\gamma} \nabla \cdot (\mathbf{u}\mathbf{B} - \mathbf{B}\mathbf{u}) = \frac{1}{\gamma} \nabla \cdot (\sigma\mu_m \nabla \mathbf{B}). \quad (7)$$

The parameter  $\chi$  allows the simulation of an effective magnetic resistivity ( $\eta = 1/\sigma\mu$ ) so as to allow different effective time scales to be used and  $\gamma$  is a preconditioning parameter introduced to speed-up convergence. The use of this equation and the selection of  $\chi$  and  $\gamma$  is discussed in depth elsewhere<sup>8</sup>. Note that this approach is only strictly valid for steady state flows and that a similar modification to the fluid flow equation allows steady state solutions to be reached much more rapidly<sup>8</sup>.

#### II.E. High Hartmann Number Flows

Flows in fusion applications are characterized by high Hartmann numbers,  $Ha$ . Such flows consist of layers where sharp gradients are present and can be resolved by using stretched grids. In its usual form, LB method uses a cubic grid, with the grid spacing such that distributions at one node propagate to adjacent nodes in one time step. An extension of the method involves using stretched grids and introducing an interpolation step in the solution of Eqs. (1) and (2) to calculate updated quantities at the mesh points, allowing efficient simulation of high  $Ha$  flows.

### III. SIMULATIONS

A basic test for MHD flows is Hartmann flow. This is the pressure-driven flow between two electrically insulating parallel plates with a magnetic field applied

perpendicular to the plates. In the case of zero field this reduces to plane Poiseuille flow.

The profile is characterized by the Hartmann number,  $Ha = BL/\sqrt{\rho\eta\nu}$  where  $L$  is a length scale, in this case taken to be half the plate separation. Fig. 2 shows the profiles of the velocity and induced field obtained with the LB model. The expected flattening of the velocity profile away from the walls is clear – for zero applied field, a parabolic profile would be present.

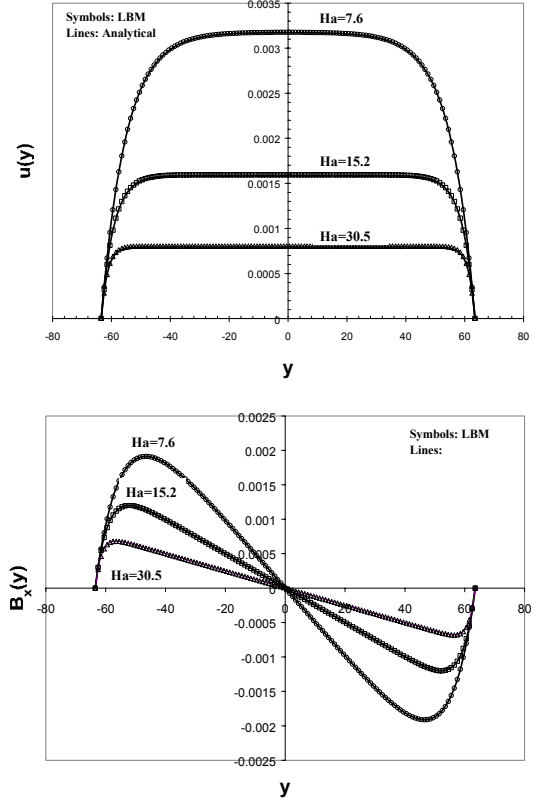


Fig. 2. Velocity (top) and induced magnetic field (bottom). Abscissa is in lattice or grid units, symbols are LB predictions and lines analytical solution.

Another case for which there is an analytical solution is the so-called Gold problem<sup>9</sup>, which is the pressure-driven flow through a cylindrical pipe with insulating walls and a field applied perpendicular to the pipe axis. Fig. 3 shows the velocity profiles in two directions and compares them with the analytical solution. The Hartmann number (based on the diameter) used was 20. Excellent agreement is seen.

A true 3-D MHD validation case is provided by the lid driven cavity. In the case presented here, the flow in a cubic box with a moving top lid with a magnetic field applied perpendicular to the direction of motion was simulated. A Reynolds number of 100 and  $Ha=45$  (based on the cube side) were used and results were compared to

predictions from a finite difference code<sup>10</sup> and plotted in Fig 4, which show good agreement.

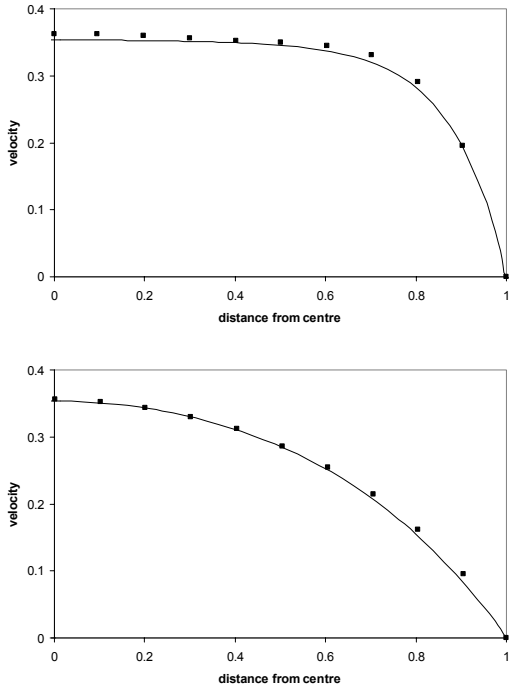


Fig. 3 Velocity profiles for directions parallel (top) and perpendicular (bottom) to applied field. Lines are LB predictions, symbols analytical solution. Ordinate is normalized such that value of 1 would correspond to peak velocity for zero applied field.

This test demonstrated the advantages of the MRT model; earlier simulations with an SRT code encountered problems with stability, severely restricting the range of parameters that could be used, but the MRT model proved much more robust.

The effect of a magnetic field on a turbulent flow was investigated by considering a pipe flow entering a magnetic field. The velocity field from an earlier simulation of pressure driven flow in a pipe was used to provide the inlet conditions. One diameter from the inlet, the magnetic field was increased linearly over two diameters to a value corresponding to a Hartmann number of 20 based on the diameter, and statistics were collected 15 diameters downstream from the entrance to the field. For this simulation, a large grid size of  $2400 \times 124 \times 124$  was used and it was executed in parallel using 32 processors.

Unresolved turbulent scales were modeled using a Smagorinsky eddy viscosity model with wall damping. Fig. 5 shows the profiles of the streamwise and radial rms turbulent fluctuations in directions parallel and perpendicular to the applied field and compares them with the case for zero field. A significant reduction in the

turbulence can be seen, which is in keeping with what is generally observed in MHD flows.

An example of a computation of high  $Ha$  flow using an interpolation supplemented LB method is shown in Fig. 6, which evidently shows excellent agreement with analytical predictions. A stretched grid with fine spacing close to the wall and coarser spacing farther out was used to simulate Hartmann flow with  $Ha=700$ .

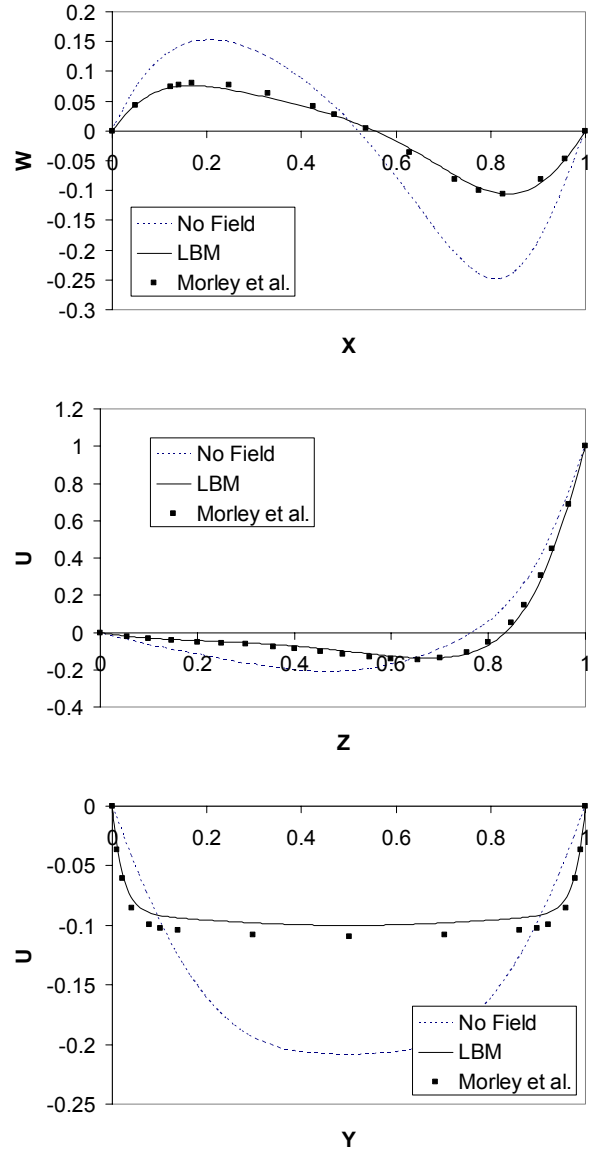


Fig. 4 Velocity profiles through centre of cavity. The lid was at  $z=1$  and moved in the  $x$ -direction with velocity unity. The magnetic field was applied in the  $y$ -direction.

#### IV. CONCLUSIONS

A set of laminar and turbulent flow simulations of MHD problems in 2D and 3D using a lattice Boltzmann method with an MRT model has been conducted. New

methods of imposing boundary conditions and resolving thin MHD layers have also been incorporated into the methodology. Results have been in good agreement with those from other sources, and the MRT model has demonstrated its superior stability compared with the SRT model.

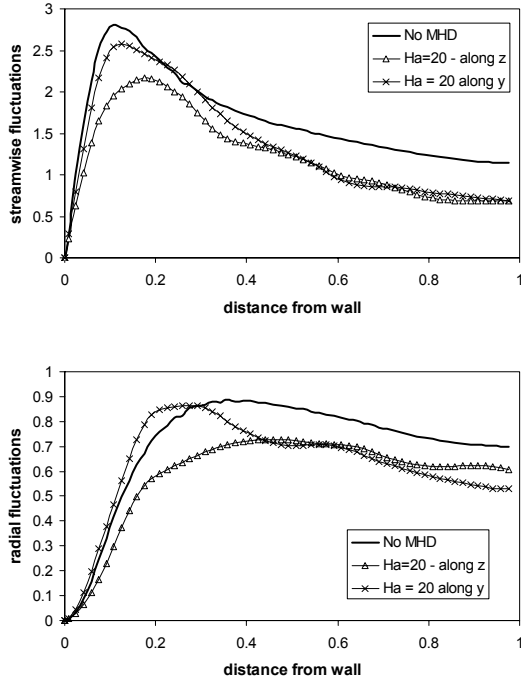


Fig. 5. Profiles of rms velocity fluctuations. Flow is in  $x$  direction and field is applied in  $z$  direction. Radius of pipe is one.

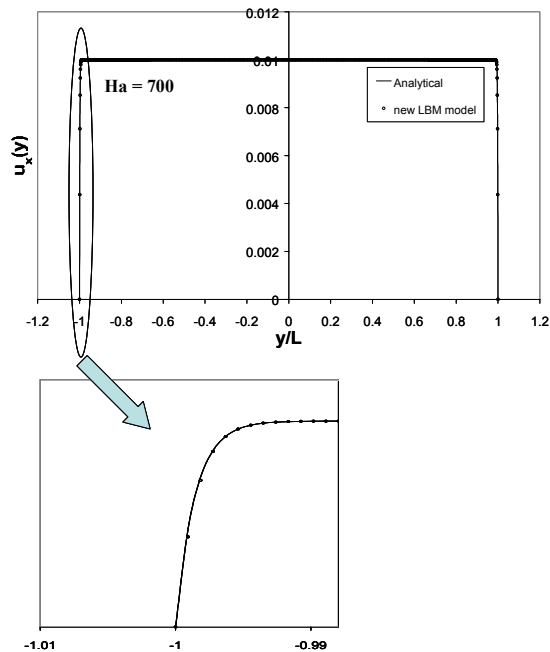


Fig. 6. Velocity profile for Hartmann flow with  $Ha=700$ .

## ACKNOWLEDGMENTS

The development of the MHD models and code was funded by the US Department of Energy (DOE) under grant No. DE-FG02-03ER83715. The work used resources of the National Energy Research Scientific Computing Center, which is supported by the Office of Science of DOE under Contract DE-AC03-76SF00098.

## REFERENCES

1. S. CHEN AND G.D. DOOLEN, "Lattice Boltzmann Method for Fluid Flows," *Annu. Rev. Fluid Mech.*, **30**, 329 (1998)
2. D. D'HUMIÈRES, I. GINZBURG, M. KRAFCHYK, P. LALLEMAND and L.-S. LUO "Multiple-Relaxation Time Lattice Boltzmann models in three dimensions," *Phil. Trans. R. Soc. Lond. A*, **360**, 437 (2002)
3. K. N. PREMNATH and J. ABRAHAM, "Three-Dimensional Multi-Relaxation-Time (MRT) Lattice-Boltzmann Models for Multiphase Flow," *J. Comp. Phys.*, in press (2006).
4. K. N. PREMNATH and M. J. PATTISON, "Generalized Lattice Boltzmann Equation with Forcing Term for LES of Bounded Turbulent Flows: Accuracy, Stability and Computational Efficiency," Submitted to *Physical Review E*
5. P. J. DELLAR, "Lattice Kinetic Schemes for Magnetohydrodynamics," *J. Comp. Phys.*, **179**, 95 (2002)
6. M. BOUZIDI, M. FIRDAOUSS and P. LALLEMAND, "Momentum Transfer of a Boltzmann-Lattice Fluid with Boundaries," *Phys. Fluids*, **13**, 3452 (2001)
7. S. CHEN, D. MARTINEZ and R. MEI, "On Boundary Conditions in lattice Boltzmann Methods," *Phys. Fluids*, **8**, 2527 (1996)
8. K. N. PREMNATH and M. J. PATTISON, "Accelerating Convergence of a Generalized Lattice Boltzmann Equation with Forcing Term to Steady State through Preconditioning and its Application for Magnetohydrodynamic Applications," Submitted to *Physical Review E*
9. R. R. GOLD, "Magnetohydrodynamic Pipe Flow. Part 1," *J. Fluid Mech.*, **13**, 505 (1962)
10. N. B. MORLEY et al., "Progress on the Modeling of Liquid Metal, Free Surface, MHD Flows for Fusion Liquid Walls," *Fusion Eng. and Des.*, **72**, 3 (2004)